# A Comparative Analysis of Single-Input Single-Output Stationarity Time and Pathloss in Suburban Environments for Vehicle-to-Infrastructure Channel Using Veneris Ray-Tracing and Real Data

Nor El Islam Dahmouni
Univ. Lille, CNRS, UMR
8520-IEMN, F-59000 Lille, France
email:norelislam.dahmouni@univ-lille.fr

Mohammed Mallik
Univ. Lille, CNRS, UMR
8520-IEMN, F-59000 Lille, France
email: mohammed.mallik@imt-nord-europe.fr

Pierre Laly
Univ. Lille, CNRS, UMR
8520-IEMN, F-59000 Lille, France
email: pierre.laly@univ-lille.fr

Esteban Egea Lopez
ITC Department,
Univ. Politécnica de Cartagena,
30202 Cartagena, Spain
email: esteban.egea@upct.es

Davy P.Gaillot
Univ. Lille, CNRS, UMR
8520-IEMN, F-59000 Lille, France
email: davy.gaillot@univ-lille.fr

***Abstract*— This paper presents a comparative study of stationarity time (Ts) of non-Wide-Sense Stationarity Uncorrelated Scattering (non-WSSUS) channel and path-loss characteristics between a Ray-tracing Veneris simulator and real-world data of Vehicle-to-Infrastructure (V2I) communication of Single-Input Single-Output (SISO) channel in a suburban environment at 5.89 GHz. The WSSUS assumption is often used to model wireless channels in order to simplify the analysis and design of communication systems. However, this assumption is not always valid for V2I channels, which can be highly dynamic and non-stationary. In this paper, a Ray-tracing simulator, namely Veneris, is used to generate synthetic V2I channel data. This data is then compared to real-world V2I channel data collected by a radio channel sounder, namely MaMIMOSA, in a suburban environment. The results show that the simulator accurately predicted the channel stationarity time of the real-world V2I channel, with a median of 560 ms compared to 550 ms for real data. Additionally, a Jensen–Shannon divergence value of 0.05 was found, suggesting a relative similarity between the simulated and real data distributions. The path-loss exponent factor was 3.5 for the simulator and 3.1 for real data.**

***Keywords-WSSUS; GLSF; CCF; V2I; 5G.***

## I. INTRODUCTION

5G is considered a major breakthrough for Vehicle-to-Infrastructure (V2I) communication, where the precise understanding of radio propagation channels is fundamental to reliable and robust wireless communication systems. These requirements are crucial for vehicular communication applications, especially for Intelligent Transportation Systems (ITS), which are developed by two main groups: The Third Generation Partnership Project (3GPP), which focuses on the Cellular-Vehicle-to-Everything (C-V2X) standard, and European Telecommunications Standards Institute (ETSI), based on IEEE 802.11p standard, known as ITS-G5 or Direct Short Range Communication (DSRC) in United States [1][2]. In addition, the crucial importance of a thorough and detailed characterization of the propagation channel becomes evident in the process of modeling and designing communication systems. A comprehensive characterization of the properties of the propagation channel leads to precise modeling, fostering the development of reliable, robust, and interoperable communication systems. The characterization of the radio propagation channel can be described using a variety of channel modeling techniques, including statistical modeling based on time-frequency domain measurement campaigns or deterministic modeling-based simulations [8].

## II. STATE OF THE ART

Ray-tracing, a deterministic modeling technique, has been widely used to characterize 5G radio channels in various environments, including urban, suburban, rural, tunnel, indoor, etc. [7][21]. For vehicular communication, numerous studies are based on Ray-tracing models for the analysis and estimation of vehicle propagation channel characteristics. These studies specifically focus on small-scale fading characteristics, signal statistics, coverage, and data rate prediction [23][24], as well as signal strength degradation [22]. Additionally, a time-varying channel modeling for low terahertz urban V2I communication is presented in [6]. In a separate study, the comparison between Ray-tracing and stochastic models is explored, particularly for urban V2I Terahertz communication channels [20].

A key feature of channel modeling, designing, and analyzing wireless propagation channels is the assumption of Wide-Sense Stationary and Uncorrelated Scattering (WSSUS). Propagation channel models conventionally incorporate the WSSUS assumptions [3][9]. The WSSUS assumptions imply that the channel mean and autocorrelation H (t, f) remain constant over time t and frequency f, or in other words, the second-order channel statistics are independent of time and frequency. This assumption simplifies transceiver design by providing simple mathematical models for the channel, enabling the use of less complex channel estimation or precoding techniques [10].

 ISBN: 978-1-68558-134-3

From a functional perspective, the analysis of non-WSSUS channel statistics could help with optimizing adaptive transmission schemes and beamforming techniques, as well as improving the overall system performance [11][12]. However, due to the high mobility of transmitters and receivers and the appearance of dynamic scatters in vehicular communication, V2I channel characteristics change rapidly over time, leading to violations of WSSUS assumptions, resulting in non-stationary behavior [9] due to the time-varying nature of Multi-Path Components (MPC). This implies that we can describe the time-varying fading process of vehicular channels by assuming that they exhibit local stationarity within a limited time and frequency range. It is therefore necessary to characterize the propagation channel and define the stationarity regions (generally the stationarity time) where the WSSUS hypothesis is valid.

A comprehensive framework for estimating time and frequency stationarity has been developed in [3][4]. The time- and frequency-dependent Generalized Local Scattering Function (GLSF) $\hat{C}(t, f, \nu, \tau)$ for non-WSSUS channels is derived by extending the scattering function $C(\tau, \upsilon)$ for WSSUS channels. The stationarity region, defined by its time and frequency stationarity limits Ts and Fs, respectively, can be derived from the GLSF using the four-dimensional Fourier transform of the GLSF, namely the Channel Correlation Function (CCF) [3]. As reported in [13] for similar scenarios, the minimum frequency stationarity is significantly greater than 150 MHz. Since ITS technologies operating at 5.9 GHz typically use bandwidths of less than 20 MHz, the radio channel is considered to be stationary in terms of frequency. Consequently, this study focuses exclusively on analyzing stationarity time Ts.

In [24], a simulator designed for non-WSSUS channels, to analyze the performance of V2X communication systems, based on Monte Carlo and Cisoid-sum models, is described in detail. Moreover, [25] presents a tapped delay line model specifically adapted to non-WSSUS Vehicle-to-Vehicle (V2V) channel scenarios. In [26], an autoregressive modeling approach for the simulation of non-stationary vehicle channels is presented, focusing on measurements to compare real data, but not directly with a deterministic Ray-tracing model. In addition, a Ray-tracing model has been developed and compared with real-world data in terms of small and large-scale channel parameters in a dense urban environment for Multiple-Input Multiple-Output (MIMO) V2I communication. The study considers the channel to be WSS and does not take into account the non-stationary behavior, as presented in [27].

Despite considerable progress in channel modeling and Ray-tracing for radio propagation channels, as well as for non-WSSUS channels in vehicular communication systems, there remains a notable gap in comprehensive comparisons between real measurement data and Ray-tracing models for non-WSSUS V2I propagation channels, particularly for the stationarity time (WSS), as identified in the current literature.

This paper presents a comparative analysis of Single-Input Single-Output (SISO) channel stationarity time and path-loss in a suburban environment at 5.89 GHz, comparing simulated Channel Transfer Functions (CTF) from the Veneris framework Ray-tracing model [16], and real measurement campaign data collected using a MaMIMOSA channel sounder [5]. The same configuration setup and scenario were employed for both simulations and measurements. The remainder of this paper is organized as follows. Section III introduces the scenario and setup. Section IV fully characterizes and compares the channel path-loss statistics between the simulated CTFs and real measurement data Additionally, it includes estimations and comparisons of the stationarity time Ts over distance for both simulated and real data. Finally, Section V concludes the discussion by summarizing key findings implications, and future perspectives.

## III. SCENARIO AND SETUP

In this section, we introduce our environment chosen for measurement and simulation on the campus of the University of Lille (ULille), France. The suburban environment consists of 3-4 story buildings spaced 5-10 m apart, with dense vegetation and trees up to 30 m high. Additionally, there is an industrial hall (8m in height) with a framework of metal portals, an overhanging sloping roof, and metal cladding. Traffic on the road was relatively low, with a maximum speed of 50 km/h, but many cars were parked along the boulevard during the drive-test. Two speed bumps, separated by 150 meters, are present in the used measurement road (Figure 1).

### *A. Real data Measurement*

The measurements were performed using the MaMIMOSA radio channel sounder with an 80 MHz bandwidth at 5.89 GHz, developed by a joint team from the ULille in France and Ghent University (UGent) in Belgium. The MaMIMOSA sounder is a real-time massive MIMO radio channel sounder that is specifically designed for V2X applications. It is equipped with a massive 64-antenna array for transmission (Tx) and up to 16 individual antennas for reception (Rx). The MaMIMOSA hardware and software capabilities allow for the sounding parameters to be freely adapted to the investigated scenario, demonstrating its versatility and flexibility [5][14]. The Tx was a massive square array of 64 antennas, but only one antenna was used in this study. The Tx was installed as a Road-Side Unit (RSU) on the sidewalk at a height of 2 meters above the ground. An omnidirectional Rx antenna was placed on the roof of a van at a height of 3 meters, as shown in Figure 2. For the mobility scenario, the van moved away from the Tx at a constant speed of 40 km/h over a total distance of 300 m, such that a Line-Of-Sight (LOS) path was always present, as shown in Figure 1. The 5.89 GHz MaMIMOSA used frequency corresponds to the frequency band offered by ITS derived from the 5.9 GHz ITS-G5 and C-V2X technologies.


Figure 1. A top view of the measurement campaign for stationarity in a suburban environment.


Figure 2. Tx-Rx antenna systems.

During the drive-test, 13670 time-varying CTFs of ~1 ms were measured over a total Tx-Rx distance of 300 m. These CTFs are organized into 5 frames of 2752 CTFs spaced by an interblock time of 1 ms. Each CTF contains 818 frequency samples spaced by eight subcarriers, which were selected across the 80 MHz bandwidth. The maximum Doppler span is ±250 Hz (corresponding to a maximum speed of 46 km/h) with a Doppler resolution of 0.181 Hz. The measurement campaign and frame configuration are detailed in [15].

### *B. Ray-tracing Data*

The Ray-tracing simulator Veneris uses the same scenario environment (Figure 3) and setup parameters of real data measured from the MaMIMOSA sounder for the simulation part, developed by Telecommunications Network Engineering Group (GIRTEL) of Polytechnic University of Cartagena (UPCT), Spain. Veneris is a comprehensive and realistic simulation environment for research on vehicular networks and cooperative automated driving, as well as a valuable tool for simulating general wireless networks requiring 3D environment-aware propagation simulation. It consists of the following components: a traffic simulator, implemented on top of the Unity game engine and including a realistic vehicle model as well as a set of driving and lane change behaviors that reproduce traffic dynamics; Opal, a Ray-launching GPU-based propagation simulator, which is an open source Ray-tracing propagation simulator for electromagnetic characterization. Opal is an integral part of the Veneris framework and can be used as a stand-alone simulator or can be integrated with the Unity game engine. It is implemented in C++ and utilizes NVIDIA OptiX, and a set of modules that facilitate bidirectional coupling with the widely used network simulator, namely Objective Modular Network Testbed in C++ (OMNET++). The functional and configurational aspects of Veneris are presented in [16][17].

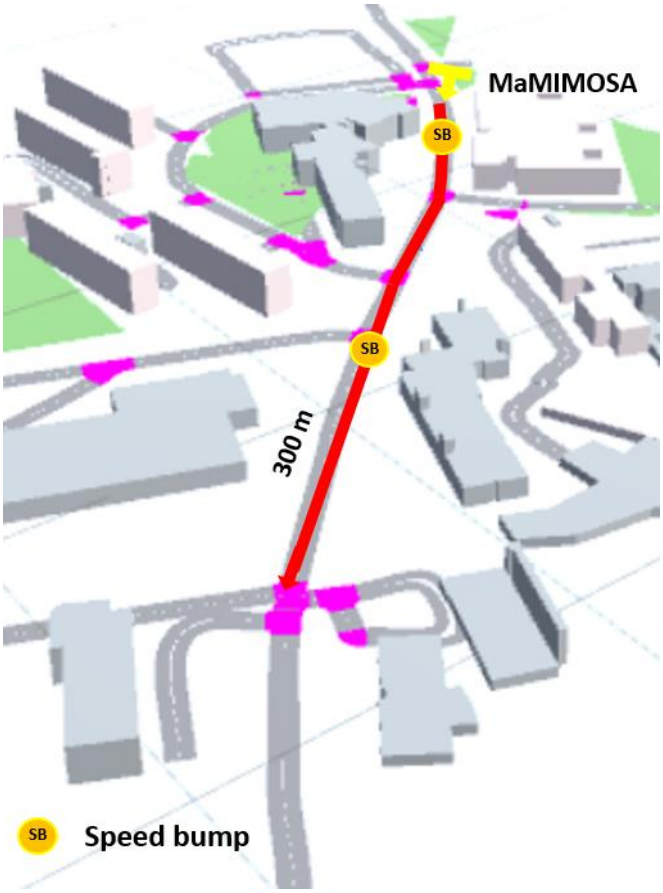


Figure 3. Veneris interface for the same scenario at 5.9 GHz.

TABLE 1. CONFIGURATION PARAMETERS

| Parameters | Configuration |
|---|---|
| Carrier frequency | 5.89 GHz |
| Measurement bandwidth | 80 MHz |
| Frequency points | 818 |
| Delay resolution | 12.5 ns |
| Doppler resolution | 0.181 Hz |
| CTF duration | ~ 1 ms |
| Total CTF number | 13760 |
| Interblock time | 1 ms |
| Transmit power | 0 dBm |
| Tx – Rx height | 2 m / 3 m |

The same setup configuration and frame were used in the Veneris configuration, with the antenna power as shown in Table 1, which summarizes the configuration parameters for both real and simulated measurements.

## IV. RESULTS AND DISCUSSION

The signal power variation of simulation data compared to real data over distance must be checked before analyzing the stationarity time and path-loss characteristics.

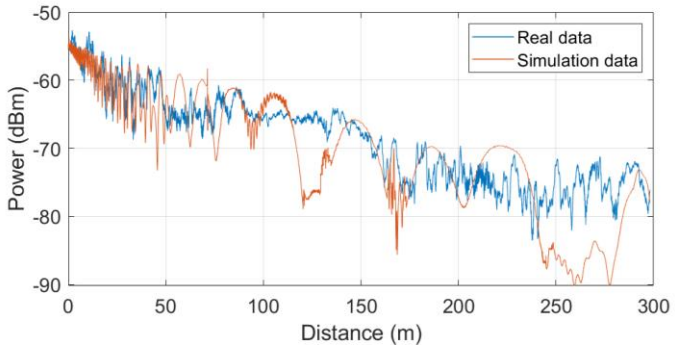


Figure 4. Received power for real and simulation data.

Figure 4 shows the received signal power in dBm for both real-world data and simulation over the Tx-Rx distance. A similar trend is observed in the received power. Within the first 50 meters, there is a power attenuation from -55 dBm to -65 dBm with rapid small-scale fluctuations attributed to the dense multipath component caused by nearby buildings. Beyond 50 meters up to 300 meters, there is a slow pronounced attenuation, ranging from -65 dBm to -80 dBm for real data and -90 dBm for simulation data. Overall, the real and simulation data are in good agreement. The main difference is that the real data is more noisy due to environmental factors. This suggests that the simulation model is accurate.

### A. *Propagation loss*

The empirical model for Path-Loss (PL) as a function of the Tx-Rx distance is given by the following expression:

$$PL(d)_{dB} = PL(d_0)_{dB} + 10 \times n \times log_{10}\left(\frac{d}{d_0}\right) \quad (1)$$

with n the path-loss attenuation exponent, which is equal to 2 in free space, and PL(d0) dB the attenuation measured at a reference distance of do=80 m based on [18].

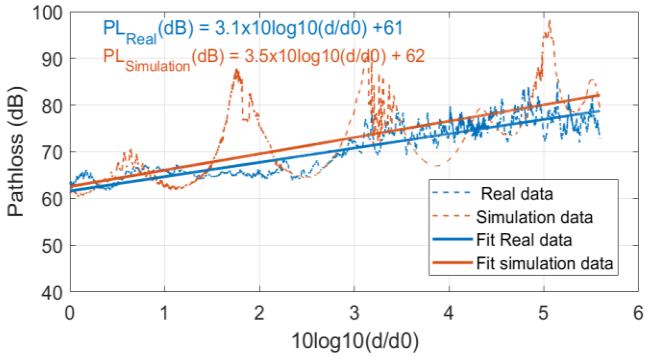


Figure 5. Path-loss fit for real-world and simulation data.

Figure 5 compares the PL plot of real-world data to the simulation plot based on equation (1). The PL exponent factor (n) is calculated using linear regression and found to be 3.1 and 3.5 for real-world and simulated PL, respectively. These results agree with previous research on similar scenarios with LOS [18][19].

### B. *Stationarity time evaluation*

Based on GLSF, and its 4D Fourier transform the CCF $A(\Delta\nu, \Delta\tau; \Delta t, \Delta f)$ [3][4].

$$A(\Delta\nu, \Delta\tau; \Delta t, \Delta f) = TF^{4D}\{\hat{C}(t, f; \nu, \tau)\} \quad (2)$$

The stationarity time Ts could be calculated as:

$$T_s = \frac{1}{\overline{\Delta\nu}} \quad (3)$$

where $\overline{\Delta\nu}$ is the Doppler correlation deduced from the CCF Doppler first moment as follows [3][4]

$$\overline{\Delta\nu} = \frac{1}{\|A\|_1} \int\int\int\int |\Delta\upsilon| A(\Delta\upsilon, \Delta\tau; \Delta t, \Delta f) d\upsilon d\tau dt df \quad (4)$$

where $\|A\|_1$ is the first norm of the CCF along the three dimensions.

The sampled CTF, the discrete representation of the GLSF CCF, and the calculation of Ts are presented and detailed in [15]. In order to estimate stationarity time over distance, we used 10 interleaved GLSF corresponding to 934.34 ms [15].

 ISBN: 978-1-68558-134-3 

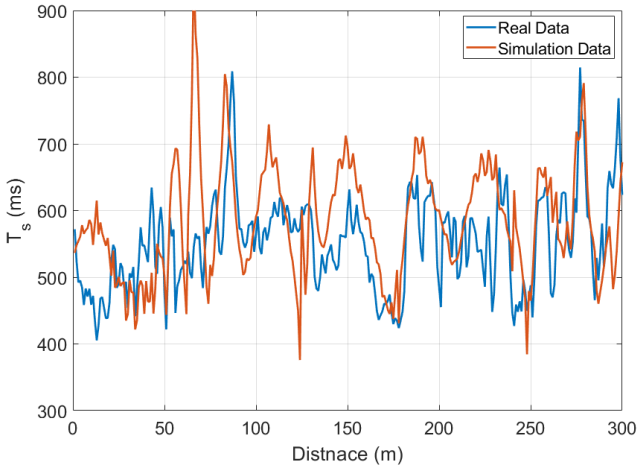


Figure 6. Stationarity time Ts over distance for real and simulated data.

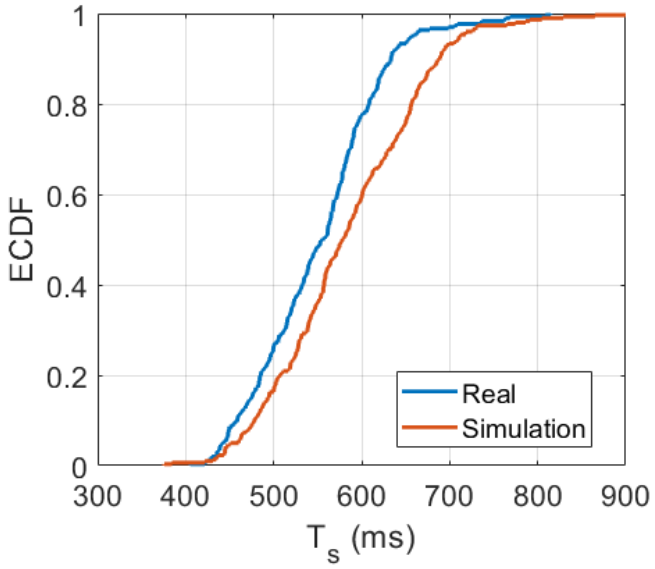


Figure 7. ECDF of Stationarity time Ts for real and simulated data.

Figures 6 and 7 show the stationarity time Ts of real and simulated data over distance and their Empirical Cumulative Distribution Function (ECDF), respectively. The results show that the real and simulated Ts follow similar trends and distributions, with medians of 550 ms and 560 ms, respectively. Additionally, using the Jensen–Shannon divergence method, which is bounded between 0 and 1 for quantifying the similarity between two probability distributions, where a value of 0 implies identical distributions, and 1 suggests maximal dissimilarity between the distributions, a value of 0.05 is found, meaning that the two probability distributions are relatively similar. This indicates that the Veneris Ray-tracing simulator can accurately reflect the physical properties of the real propagation channel. Table 2 summarizes some statistics of Ts.

TABLE 2. COMPARISON OF STATIONARITY TIME BETWEEN REAL DATA AND SIMULATION

| | **Median** | **Std** | **Min** |
|---|---|---|---|
| **Ts real** | 550 ms | 74 ms | 418 ms |
| **Ts simulation** | 560 ms | 86 ms | 396 ms |

## V. Conclusion & Future Work

This paper presented a comparative study of non-WSSUS SISO channel stationarity time and path-loss characteristics between the Veneris Ray-tracing simulator and real-world data of V2I communication in a suburban environment at 5.89 GHz. The simulator accurately predicted the channel stationarity time of the real-world V2I channel, with a median of 560 ms compared to 550 ms for real data. Furthermore, a Jensen–Shannon divergence value of 0.05 was found, indicating a relative similarity between the simulated and real data distributions. The path-loss exponent factor was 3.5 for the simulator and 3.1 for real data. These results suggest that the simulator can accurately reflect the stochastic physical properties of the channel, making it a reliable tool for evaluating the performance of V2I communication systems in different suburban environments.

In future work, we will extend this paper by comparing the simulator in massive MIMO array configurations to evaluate the statistical spatial behavior of the stationarity time Ts across the massive array and the angular properties of the MPCs, such as the Angles of Arrival (AoA) and the Angles of Departure (AoD) values and spreads.

## Acknowledgment

This work has been partially funded by Grant PID2020-112675RB-C41 funded by (MCIN/AEI/10.13039/50110001103). E. Egea-Lopez thanks the European Association on Antennas and Propagation (EurAAP) for funding the STSM under which this work was done.

## References

[1] F. Arena, G. Pau, and A. Severino, "A review on IEEE 802.11 p for intelligent transportation systems," Journal of Sensor and Actuator Networks, vol. 9, no. 2, pp. 22, 2020.

[2] A. Alalewi, I. Dayoub, and S. Cherkaoui, "On 5G-V2X use cases and enabling technologies: A comprehensive survey," IEEE Access, vol. 9, pp. 107710-107737, 2021.

[3] G. Matz, "On non-WSSUS wireless fading channels," IEEE Transactions on Wireless Communications, vol. 4, no. 5, pp. 2465-2478, 2005.

[4] G. Matz, "Doubly underspread non-WSSUS channels: Analysis and estimation of channel statistics," in 2003 4th IEEE Workshop on Signal Processing Advances in Wireless Communications-SPAWC 2003 (IEEE Cat. No. 03EX689), pp. 190-194, 2003.

[5] D. P. Gaillot et al., "Measurement of the V2I massive radio channel with the MaMIMOSA sounder in a suburban environment," in 2021 15th European Conference on Antennas and Propagation (EuCAP), pp. 1-4, 2021.

[6] Y. Chen and C. Han, "Time-varying channel modeling for low-terahertz urban vehicle-to-infrastructure communications," in 2019 IEEE Global Communications Conference (GLOBECOM), pp. 1-6, 2019.

[7] M. Ghaddar, J. M. García-Pardo, I. B. Mabrouk, M. Lienard, and P. Degauque, "UTD-Based Ray Tracing MIMO Channel Modeling for the Next Generation Communications within

Underground Tunnels," IEEE Transactions on Antennas and Propagation, 2023.

[8] G. Tiberi et al., "An efficient ray tracing propagation simulator for analyzing ultrawideband channels," in 2007 IEEE International Conference on Ultra-Wideband, pp. 794-799, 2007.

[9] F. Hlawatsch and G. Matz, "Wireless communications over rapidly time-varying channels," Academic Press, 2011.

[10] A. F. Molisch, "Wireless communications," vol. 34, John Wiley & Sons, 2012.

[11] O. Renaudin, V.-M. Kolmonen, P. Vainikainen, and C. Oestges, "Non-stationary narrowband MIMO inter-vehicle channel characterization in the 5-GHz band," IEEE Transactions on Vehicular Technology, vol. 59, no. 4, pp. 2007-2015, 2010.

[12] U.A.K. Chude-Okonkwo, R. Ngah, and T. Abd Rahman, "Time-scale domain characterization of non-WSSUS wideband channels," EURASIP Journal on Advances in Signal Processing, vol. 2011, no. 1, pp. 1-20, 2011.

[13] L. Bernadó, T. Zemen, F. Tufvesson, A. F. Molisch, and C.F. Mecklenbräuker, "The (in-) validity of the WSSUS assumption in vehicular radio channels," in 2012 IEEE 23rd International Symposium on Personal, Indoor and Mobile Radio Communications (PIMRC), pp. 1757-1762, 2012.

[14] P. Laly et al., "Massive radio channel sounder architecture for 5G mobility scenarios: MaMIMOSA," in 2020 14th European Conference on Antennas and Propagation (EuCAP), pp. 1-5, 2020

[15] N. E. I. Dahmouni et al., "On the Stationarity Time of a Vehicle-to-Infrastructure Massive Radio Channel in a Line-of-Sight Suburban Environment," Sensors, vol. 22, no. 21, p. 8420, 2022.

[16] E. Egea-Lopez, F. Losilla, J. Pascual-Garcia, and J. M. Molina-Garcia-Pardo, "Vehicular networks simulation with realistic physics," IEEE Access, vol. 7, pp. 44021-44036, 2019.

[17] E. Egea-Lopez, J.M. Molina-Garcia-Pardo, M. Lienard, and P. Degauque, "Opal: An open source ray-tracing propagation simulator for electromagnetic characterization," Plos One, vol. 16, no. 11, p. e0260060, 2021.

[18] T. S. Rappaport, K. Blankenship, and H. Xu, "Propagation and radio system design issues in mobile radio systems for the glomo project," Virginia Polytechnic Institute and State University, 1997.

[19] N. H. Talib et al., "An efficient algorithm for large-scale RFID network planning," in 2019 IEEE Jordan International Joint Conference on Electrical Engineering and Information Technology (JEEIT), pp. 519-524, 2019.

[20] Y. Li, Y. Chen, D. Yan, K. Guan, C. Han, "Channel Characterization and Ray-Tracing Assisted Stochastic Modeling for Urban Vehicle-to-Infrastructure Terahertz Communications," IEEE Transactions on Vehicular Technology, vol. 72, no. 3, pp. 2748-2763, 2022.

[21] D. He et al., "The design and applications of high-performance ray-tracing simulation platform for 5G and beyond wireless communications: A tutorial," IEEE Communications Surveys & Tutorials, vol. 21, no. 1, pp. 10-27, 2018.

[22] B. Colo, A. Fouda, and A. S. Ibrahim, "Ray tracing simulations in millimeter-wave vehicular communications," in 2019 IEEE 30th Annual International Symposium on Personal, Indoor and Mobile Radio Communications (PIMRC), pp. 1-4, 2019.

[23] D. Kong et al., "V2I mmWave Connectivity for Highway scenarios," in 2018 IEEE 29th annual international symposium on personal, indoor and mobile radio communications (PIMRC), pp. 111-116, 2018.

[24] J. Zhao, L. Xiong, D. He, and J. Du, "Channel characteristics of rail traffic tunnel scenarios based on ray-tracing simulator," Wireless Communications and Mobile Computing, vol. 2018, 2018.

[25] Y. Li et al., "A TDL based non-WSSUS vehicle-to-vehicle channel model," International Journal of Antennas and Propagation, vol. 2013, 2013.

[26] M. Yusuf et al., "Autoregressive Modeling Approach for Non-Stationary Vehicular Channel Simulation," IEEE Transactions on Vehicular Technology, vol. 71, no. 2, pp. 1124-1131, 2021.

[27] K. H. Ng, E. K. Tameh, A. Doufexi, M. Hunukumbure, and A. R. Nix, "Efficient multielement ray tracing with site-specific comparisons using measured MIMO channel data," IEEE Trans. Veh. Technol., vol. 56, no. 3, pp. 1019-1032, 2007.

 ISBN: 978-1-68558-134-3 